Monte Carlo Simulation of Percolation Phenomena for Direct Current in Large Square Matrices

Pawel Zukowski [1], Pawel Okal [2], Konrad Kierczynski [2,*], Przemyslaw Rogalski [2], Vitalii Bondariev [2] and Alexander D. Pogrebnjak [3]

[1] Department of Economics, Vincent Pol University in Lublin, 2, Choiny Str., 20-816 Lublin, Poland; zukowski50pawel@gmail.com

[2] Department of Electrical Devices and High Voltage Technology, Faculty of Electrical Engineering and Computer Science, Lublin University of Technology, 38A, Nadbystrzycka Str., 20-618 Lublin, Poland; p.okal@pollub.pl (P.O.); p.rogalski@pollub.pl (P.R.); v.bondariev@pollub.pl (V.B.)

[3] Faculty of Electronics and Information Technology, Sumy State University, 2, Rymskogo-Korsakova Str., 40007 Sumy, Ukraine; alexp@i.ua

* Correspondence: k.kierczynski@pollub.pl; Tel.: +48-81-538-4328

Abstract: In this study, an in-depth analysis of the percolation phenomenon for square matrices with dimensions from $L = 50$ to 600 for a sample number of 5×10^4 was performed using Monte Carlo computer simulations. The percolation threshold value was defined as the number of conductive nodes remaining in the matrix before drawing the node interrupting the last percolation channel, in connection with the overall count of nodes within the matrix. The distributions of percolation threshold values were found to be normal distributions. The dependencies of the expected value (mean) of the percolation threshold and the standard deviation of the dimensions of the matrix were determined. It was established that the standard deviation decreased with the increase in matrix dimensions, ranging from 0.0262253 for a matrix with $L = 50$ to 0.0044160 for $L = 600$, which is almost six-fold lower. The mean value of the percolation threshold was practically constant and amounted to approximately 0.5927. The analysis involved not only the spatial distributions of nodes interrupting the percolation channels but also the overall patterns of node interruption in the matrix. The distributions revealed an edge phenomenon within the matrices, characterized by the maximum concentration of nodes interrupting the final percolation channel occurring at the center of the matrix. As they approached the edge of the matrix, their concentration decreased. It was established that increasing the dimensions of the matrix slowed down the rate of decrease in the number of nodes towards the edge. In doing so, the area in which values close to the maximum occurred was expanded. Based on the approximation of the experimental results, formulas were determined describing the spatial distributions of the nodes interrupting the last percolation channel and the values of the standard deviation from the matrix dimensions. The relationships obtained showed that with increasing matrix dimensions, the edge phenomenon should gradually disappear, and the percolation threshold standard deviation values caused by it will tend towards zero.

Keywords: percolation phenomenon; percolation threshold; uncertainty of measurement; metrological approach; computer simulation; Monte Carlo method

1. Introduction

The phenomenon of percolation, research of which has been rapidly gaining momentum since the 1950s, is used in the description of various systems and phenomena [1–9]. It is a critical phenomenon describing phase transitions of the second type, the general idea of which is that in any medium made of two phases, elements of one phase that are independent due to random factors create a more complicated structure, which results in a change in the macroscopic properties of the entire medium because of a change in the concentration of the dispersed phase [10]. Thus, percolation theory encompasses models

for both planar and three-dimensional random processes, along with the impact of their interplay. It serves to characterize systems featuring stochastic geometry and systems that are topologically disorganized. This is illustrated by the model of S.R. Broadbent and J.M. Hammersley, who, as precursors of the percolation theory, created the first stochastic model, which was an arbitrary network with a finite number of nodes [11]. Nodes in such a model are assigned two states, open or closed, and their number is marked as x. The probability p is the probability of their arrangement; therefore, there is a value of x for which the probability of percolation is non-zero, because the number of nodes creating the percolation channel is sufficient to create a continuous connection. This value is designated x_c and is called the percolation threshold [12,13]. Due to the adopted assumptions of the model, percolation phenomena are divided into two groups. If the states between nodes are assigned to the connections between them, then it is a bond percolation, while when the states are assigned to the entire nodes, it is a site percolation [14]. Due to the random nature of the phenomenon, the percolation threshold cannot be determined based on a single modeling.

Because in both cases the centers are discrete sets, their analysis is possible using computer simulation based on the Monte Carlo method [15]. Over an extended duration, investigations employing the simulation of the percolation phenomenon in two-dimensional networks exhibiting translational symmetry have been employed for the theoretical analysis of this phenomenon and, in certain instances, for its visual representation. Subsequent investigations in this realm have involved the increasingly precise determination of the percolation threshold value [16–21]. The record result for the uncertainty of determining the percolation threshold for square networks was obtained in publication [22], the value of which is approximately 10^{-8}. Nevertheless, such a high level of precision is unnecessary, for instance, in the analysis of experimental results, where an uncertainty of approximately 10^{-3} or 0.1% is sufficient.

In recent decades, a new field of materials has emerged, called 2D materials. These are two-dimensional materials with translational symmetry, consisting of flat lattices ranging in thickness from one to several atomic dimensions. Such materials are graphene, MXenes and a few others; see, for example, [23–38]. The examination of the dispersion of inclusions leading to conductivity through tunneling aligns precisely with the investigation of the percolation phenomenon in two-dimensional matrices exhibiting translational symmetry. Consequently, studying percolation in 2D lattice systems with translational symmetry, coupled with the exploration and advancement of technologies for fabricating 2D materials, could gain both applicative and practice attributes.

In the study cited as reference [39], researchers employed Monte Carlo computer simulations to investigate the percolation phenomenon in square matrices of different sizes. They analyzed a vast range of samples, varying from 5×10^4 to 5×10^6. Their findings revealed that the average percolation threshold remained nearly constant across different matrix sizes. However, a notable decrease, over two-fold, was observed in the standard deviation as the size of the matrix increased. In [40], it was established that in matrices with dimensions $L = 55$, 101 and 151, an edge phenomenon manifests, characterized by a reduction in the concentration of nodes forming a percolation channel as one approaches the edge of the matrix.

The aim of this work was an in-depth analysis of the parameters of the edge phenomenon for the percolation threshold in square matrices over a wide range of dimensions, from relatively small ones of $L = 50$ to large ones of $L = 600$, with the number of samples being 5×10^4 for each matrix. The residual goals of the work were:

- the determination of the two-dimensional spatial distributions of node coordinates interrupting the last percolation channel for square base matrices with dimensions from $L = 50$ to 600 for 5×10^4 samples;
- the determination of a formula describing the influence of matrix dimensions on the standard deviation values, based on the approximation of experimental results;

- the determination of the relationships describing the spatial distribution of nodes interrupting the last percolation channel depending on the dimensions of the matrix;
- the determination of the formula describing the maximum rate of reduction in the concentration of nodes interrupting the last percolation channel towards the edge of the matrix;
- the determination of the correlation between the intensity of the edge phenomenon for the distribution of nodes interrupting the last percolation channel and the value of the standard deviation of the percolation threshold depending on the dimensions of the matrix.

2. Research Method

An in-depth analysis of the parameters of the edge phenomenon for the percolation threshold of square matrices in a wide range of dimensions, which was the aim of this work, was performed using computer simulation. Both the algorithm itself and the program were described in [39]. Generally, the algorithm was based on set theory where nodes were described using Cartesian coordinates. Using a pseudorandom number generator, the program sequentially changed the states of the nodes while controlling and recording the evolution of cluster formation and the overall geometry of the simulated matrix. Moreover, when an infinite cluster was obtained, it recorded information about the percolation threshold value and the coordinates of the critical nodes that formed the percolation channel for further analysis. This process was repeated independently 5×10^4 times for matrices of size $L = 50, 75, 100, 125, 150, 175, 200, 250, 300, 350, 400, 500$ and 600.

3. Research and Analysis of Basic Percolation Parameters Depending on the Dimensions of the Matrix

3.1. Determination of the Parameters of the Probability Distribution of Percolation Thresholds Depending on the Dimensions of the Matrix

In this work, simulations were performed for matrices from $L = 50$ to $L = 200$ with a step of 25, from $L = 200$ to $L = 400$ with a step of 50, and for $L = 500$ and 600. In article [39], it was found that the standard deviation values of the percolation threshold for the range of simulation samples below 10^4 were unsatisfactory. Their stabilization occurred for sample numbers above 10^4. Therefore, for the purposes of the present work, the number of samples for each matrix was chosen to be 5×10^4. Based on simulations for each sample, the percolation threshold value and the coordinates of the node interrupting the final percolation channel were determined. The standard deviation value was also determined for each matrix. Based on the values obtained, histograms of the distribution of percolation threshold values were made and normal distributions were determined. These results are shown for selected matrices in Figures 1–3. Figure 4 shows the normal distributions for selected matrices with dimensions ranging from 50 to 600.

Figure 1 shows that there was an edge phenomenon in the matrices, such that the nodes that formed the percolation threshold were concentrated in the central part of the matrix. As each edge was approached, the number of these nodes decreased. In the central part, the number of nodes forming the percolation threshold was about an order of magnitude higher than that near the edge.

From an analysis of Figure 4 and Table 1, it is evident that the average percolation threshold value (indicated by the peak of the waveforms) remained relatively unchanged, considering the uncertainty range, regardless of the matrix size. Conversely, the standard deviation value (reflected in the breadth of the waveforms) showed a decreasing trend as the dimensions of the matrix increased. This resulted in an increase in the maximum value of the normal distributions.
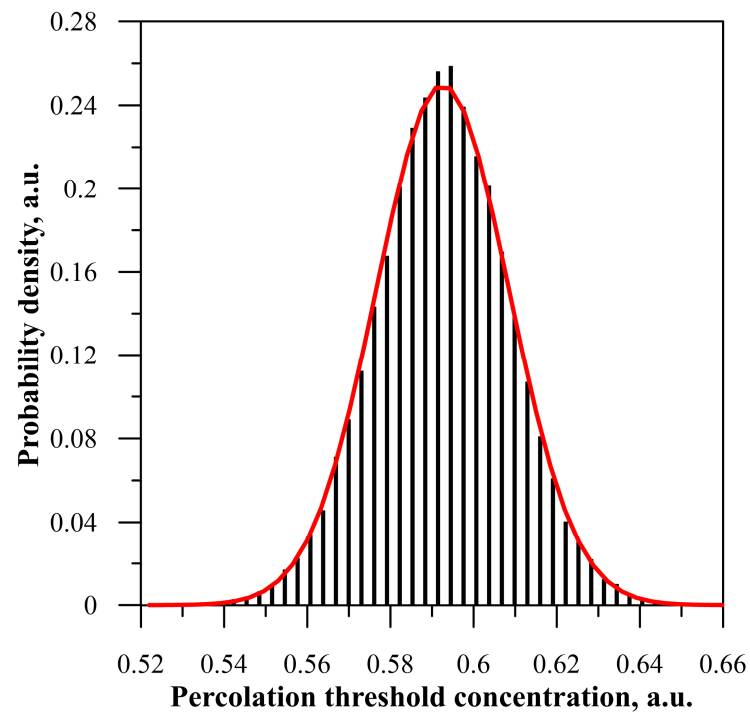
Figure 1. A graph showing the frequency distribution of percolation threshold values for a set of 5×10^4 samples in a matrix with dimensions $L = 100$, accompanied by a curve representing the normal distribution, depicted as a solid line.
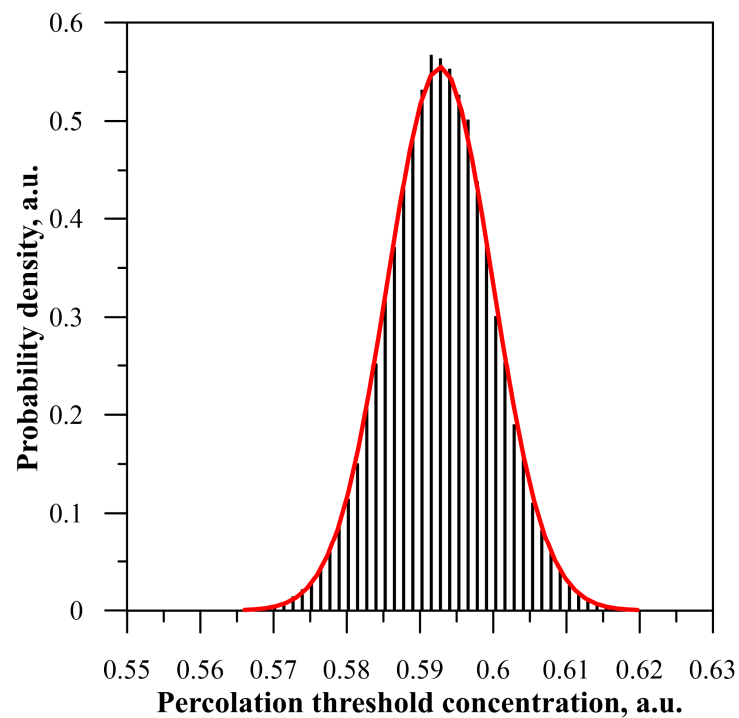

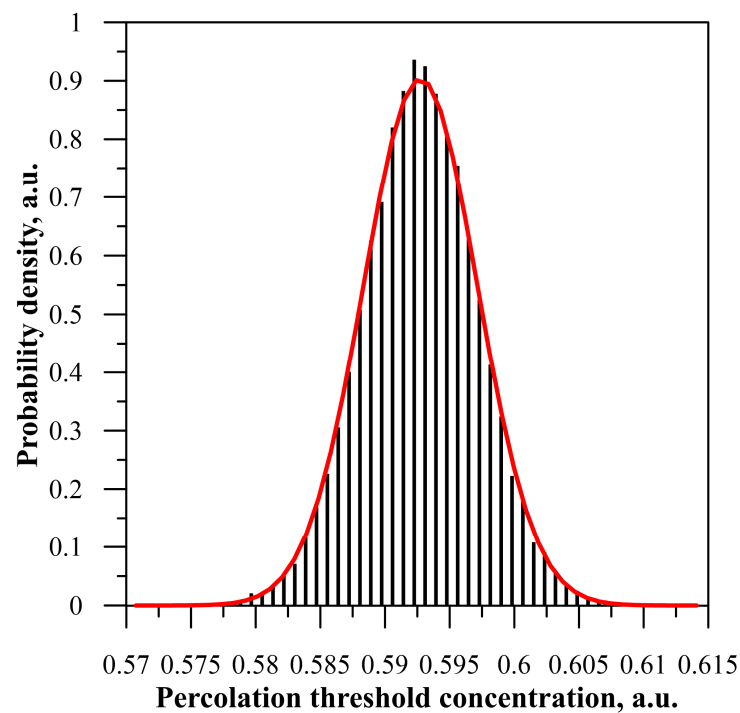**Figure 2.** A graph showing the frequency distribution of percolation threshold values for a set of 5×10^4 samples in a matrix with dimensions $L = 300$, accompanied by a curve representing the normal distribution, depicted as a solid line.

Figure 3. A graph showing the frequency distribution of percolation threshold values for a set of 5×10^4 samples in a matrix with dimensions $L = 600$, accompanied by a curve representing the normal distribution, depicted as a solid line.

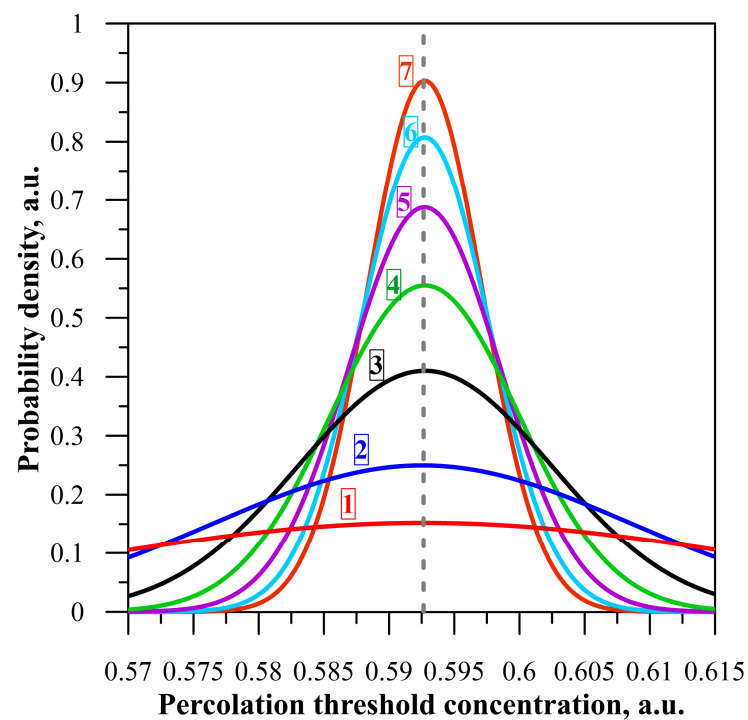**Figure 4.** Normal distributions for L: 1—50, 2—100, 3—200, 4—300, 5—400, 6—500 and 7—600. Number of samples: 5×10^4.

Table 1. Dependence of percolation threshold mean value, standard deviation and coefficient of determination R^2 on matrix dimensions for 5×10^4 samples.

Matrix Dimensions L	Percolation Threshold Value, a.u.	Standard Deviation, a.u.	Coefficient of Determination R^2, a.u.
50	0.592187	0.0262253	0.99392
75	0.592663	0.0197870	0.99476
100	0.592443	0.0159748	0.99631
125	0.592767	0.0137418	0.99679
150	0.592616	0.0119424	0.99826
175	0.592718	0.0106823	0.99733
200	0.592726	0.0097261	0.99805
250	0.592751	0.0082911	0.99775
300	0.592732	0.0071884	0.99811
350	0.592717	0.0063989	0.99894
400	0.592713	0.0058001	0.99786
500	0.592726	0.0049406	0.99813
600	0.592738	0.0044160	0.99771

Using least-squares estimation, the R^2 coefficients of determination were determined for the normal distribution approximation of the percolation threshold values for matrices of different dimensions. The value of the R^2 coefficient for all matrices was greater than 0.993. This demonstrated the high accuracy of the approximation of the results using a normal distribution and that the percolation threshold values were random values. The results obtained are shown in Table 1. From the analysis of the dependence of the mean value of the percolation threshold on the matrix dimensions shown in Figure 5, it can be seen that for matrix dimensions of $L \leq 250$, the mean value varied from about 0.592187 to about 0.592767, which is about ± 0.00058 or $\pm 0.0979\%$. For values of $L > 250$ and above, the waveform became close to steady state and the variation decreased and ranged from 0.592712 to 0.592737, which is only ± 0.000025 or $\pm 0.0042\%$. This means that for $L > 250$, the fluctuations in the mean value of the percolation threshold decreased by more than 20-fold compared to the range with lower matrix sizes and were virtually negligible.
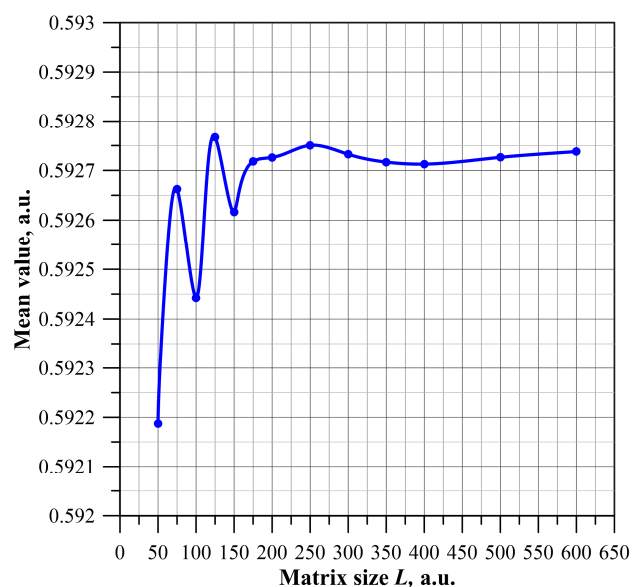

Figure 5. Dependence of mean value on matrix size for 5×10^4 samples.

Figure 6 illustrates how the value of the percolation threshold and its standard deviation varied with the size of the matrix. The data presented in Figure 6 clearly indicate that the value of the percolation threshold remained largely unaffected by changes in the

dimensions of the matrix. In contrast, the standard deviation and the associated uncertainty of the percolation threshold decreased with increasing matrix dimensions.
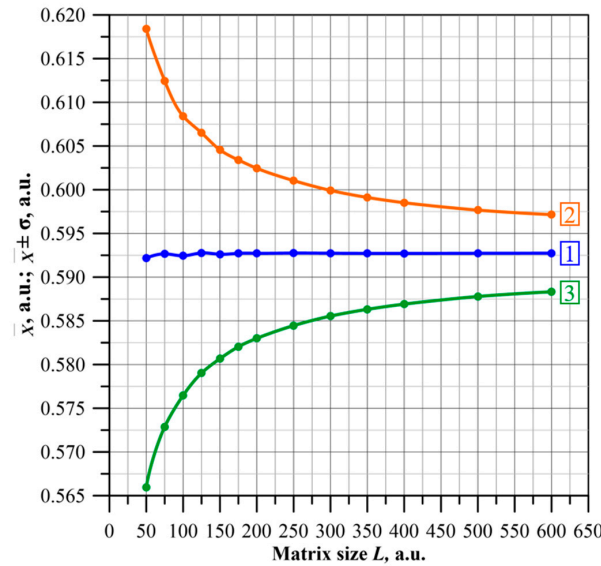

Figure 6. Dependence of percolation threshold mean value (1), mean + standard deviation (2) and mean − standard deviation (3) on matrix size L for 5×10^4 samples.

Figure 7 shows the dependence of the standard deviation on the matrix dimensions. From it, the dependence of the power approximation function on the matrix dimension L was obtained, given by the formula:

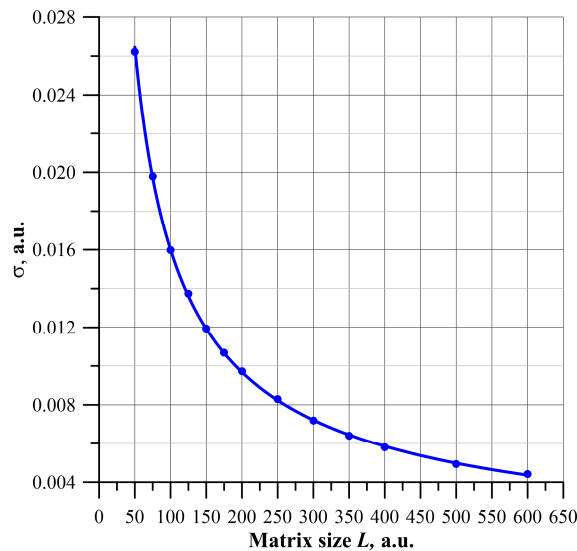$$\sigma(L) \approx 0.045 L^{-0.75}. \tag{1}$$

Figure 7. Dependence of the standard deviation on matrix size L for 5×10^4 samples.

The quality of the approximation, shown in Figure 7, is very good, as evidenced by the value of the coefficient of determination $R^2 = 0.99982$. This value is close to unity, and the difference between unity and R^2 is only 0.00018. It can be seen from Formula (1) that the standard deviation tends towards zero as the matrix dimension L increases.

3.2. The Edge Phenomenon of Node Coordinates Interrupting the Last Percolation Channel

Figure 6 demonstrates that the average percolation threshold value remained essentially constant, regardless of the size of the matrix. Conversely, as depicted in Figure 7, the

standard deviation value showed a significant decrease as the dimensions of the matrix increased. Figure 7 shows that with an increase in matrix dimensions from 50 to 600, the standard deviation decreased by almost six-fold. In order to determine the cause of the decrease in standard deviation with increasing matrix dimensions, spatial distributions of the nodes interrupting the last percolation channel were developed.

For this purpose, the coordinates of the node that interrupted the last percolation channel were determined from a computer simulation for each successive sample. To achieve this, the computational simulations were employed to ascertain the coordinates of the node responsible for interrupting the final percolation channel in each consecutive sample. This node, also referred to as the node that formed the percolation threshold, caused the DC flow to disappear between the upper and lower edges of the matrix when it was removed.

A constant number of samples with increasing matrix dimensions resulted in a decreasing number of non-conducting nodes, interrupting the last percolation channel, at individual nodes of the square matrix. This made it impossible to compare the simulation results for matrices of different dimensions. In order to compare the density distributions of the nodes forming the percolation threshold, determined for matrices of different sizes, so-called containers were used. A container is an area containing a certain number of nodes of a network, in our case, a square network. As the dimensions of the matrix increase, the dimensions of the container increase proportionally to them. This causes the number of containers to remain constant in matrices of different dimensions. Therefore, as the matrix dimensions increase, the average number of nodes, interrupting the last percolation channel going into a container remains constant. This allows for a comparison of the spatial distributions of these nodes for matrices of different sizes. The symmetry of the square matrices was taken into account when determining the dimensions of the containers.

In this paper, the spatial distributions of the nodes forming the percolation threshold located in containers were determined for matrices with L dimensions of 50, 100, 200, 300, 400, 500 and 600. The distributions were made in the form of heat maps, often used for this purpose [x, y, z, n]. Figures 8–10 show, as examples, the distributions for matrices of dimensions 50, 200 and 500. The figures illustrate that the nodes constituting the percolation threshold were concentrated in the central part of the matrix. Approaching the edges, both top and side, the number of these nodes decreased. The edge phenomenon of the distribution of nodes forming the percolation threshold, observed in [40] for matrices of dimensions 55, 101 and 151, was present.
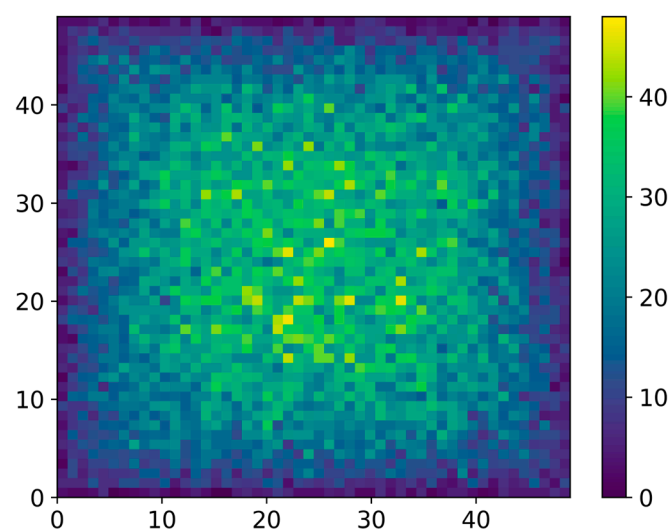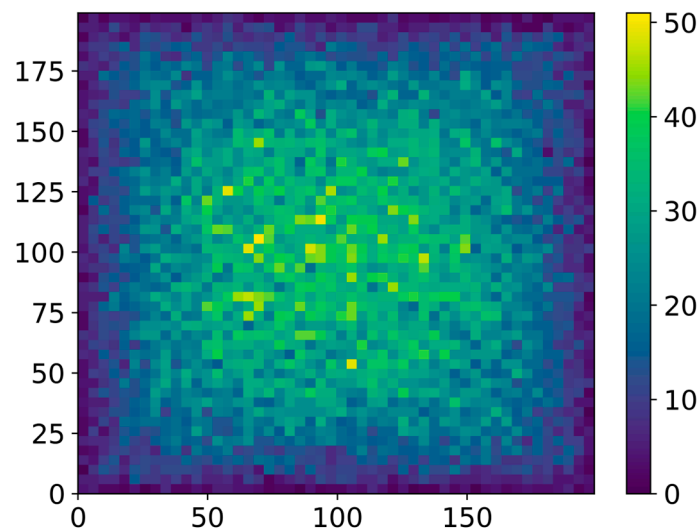

Figure 8. Two-dimensional heat map of the dependence of the number of non-conductive nodes interrupting the last percolation channel for the coordinates of the nodes of a matrix of dimensions $L = 50$ for 5×10^4 samples.
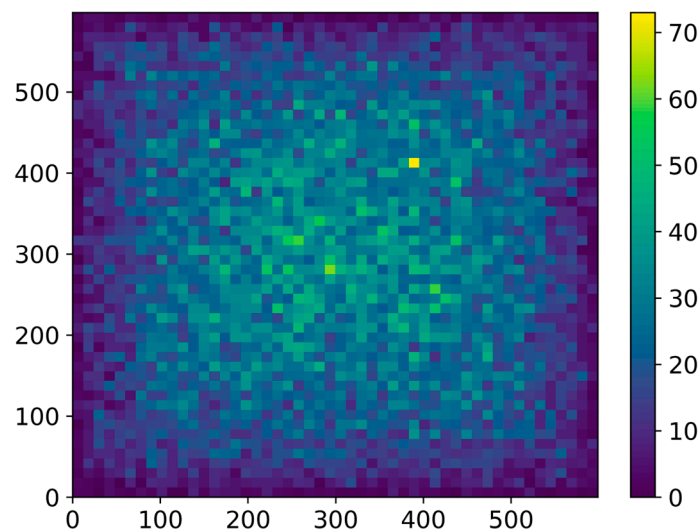
Figure 9. Two-dimensional heat map of the dependence of the number of non-conductive nodes interrupting the last percolation channel for the coordinates of the containers of a matrix of dimensions $L = 200$ for 5×10^4 samples.

Figure 10. Two-dimensional heat map of the dependence of the number of non-conductive nodes interrupting the last percolation channel for the coordinates of the containers of a matrix of dimensions $L = 600$ for 5×10^4 samples.

In order to accurately analyze the distribution of nodes forming the percolation threshold, graphs of the dependence of the number of nodes forming the percolation threshold on container coordinates were developed. Figure 11 shows the simulation results as points and polynomial approximations as solid lines.

The computational and approximation results showed that for all matrices, the maximum was located in the center of the matrix, and that the values at the maximum for the different matrices were virtually the same. As the matrix edge was approached, there was a reduction in the concentration of nodes that interrupted the final percolation channel located within the confines of the containers. Increasing the size of the matrix slowed down the rate of decrease in the concentration of nodes interrupting the last percolation channel towards the edge. It can be seen from Figure 11 that as the matrix dimensions increased, the area in which the number of nodes forming the percolation threshold was close to the maximum value increased.
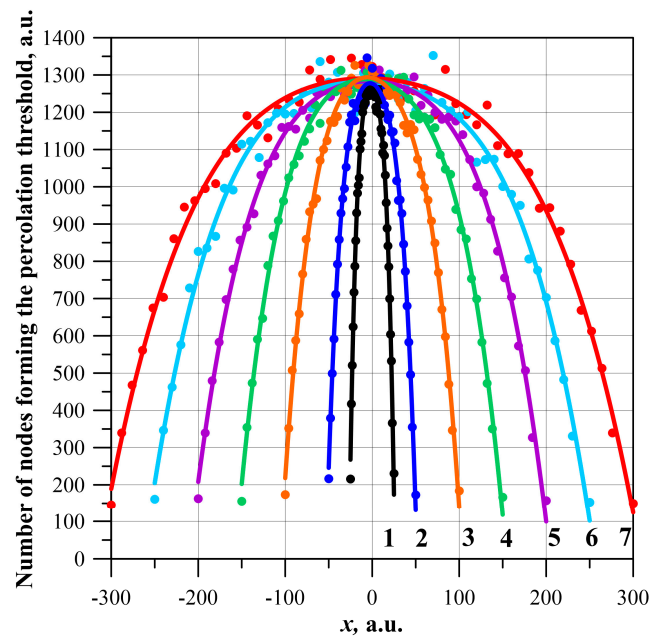
Figure 11. Number of nodes forming the percolation threshold in containers, distributed along the axes for matrix dimensions: 1—50, 2—100, 3—200, 4—300, 5—400, 6—500, 7—600 and polynomial approximations. Number of samples: 5×10^4.

The mean value of the R^2 determination coefficients for the polynomial approximations for all individuals was $R^2 \approx (0.992157 \pm 0.003208)$. This value indicated a good quality of fit of the approximating waveforms to the simulation results.

The rate of change of the distribution function of the number of nodes forming the percolation threshold was characterized by the derivative. Based on the approximating functions (Figure 11), the derivatives were calculated for the different dimensions of the matrix, as shown in Figure 12.
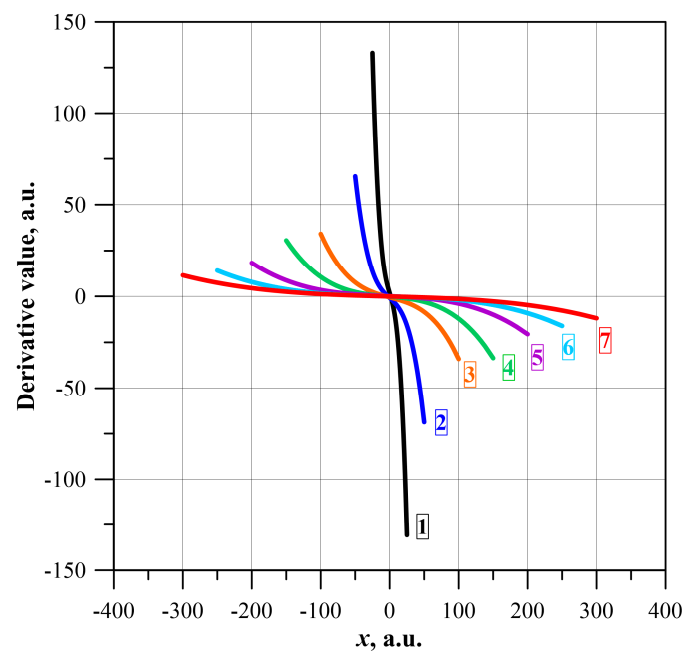

Figure 12. Plot of derivatives of the approximating function for the dimensions of the matrices: 1—50, 2—100, 3—200, 4—300, 5—400, 6—500 and 7—600.

It can be seen from Figure 12 that as the dimensions of the matrix increased, the value of the derivative decreases and becomes flatter. The largest value of each derivative is obtained at the side edge. Figure 13 shows the dependence of the modulus of the derivative value at the right-side edge on the dimensions of the matrix. The continuous line shows the waveform approximating this relationship.
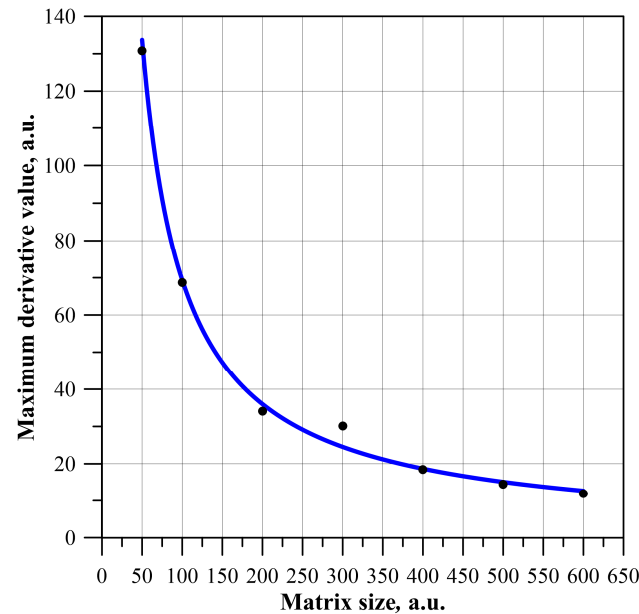

Figure 13. Dependence of the modulus of the maximum derived value on the matrix size *L*.

It can be seen from Figure 13 that the modulus of the maximum value of the derivatives decreased as the dimension *L* of the matrix increased.

The R^2 value of the approximating waveform from Figure 13 was close to unity and was 0.9863. This indicated good quality of the approximation. The equation of the approximating function was also obtained:

$$y \approx 5423 L^{-1} \tag{2}$$

As can be seen from the figures above, the highest concentration of nodes interrupting the last percolation channel was near the center of the matrix. The further away from the center, the lower the content of nodes. As depicted in the aforementioned figures, the highest concentration of nodes interrupting the final percolation channel was situated in close proximity to the matrix's center. Moving away from the center resulted in a gradual decline in node concentration. This means that, for a finite-dimensional matrix, there was an edge phenomenon in that, as the edge of the matrix was approached, the concentration of nodes interrupting the last percolation channel decreased. As the dimensions of the matrix increase, there was a slowing down of the tendency of the concentration of nodes interrupting the last percolation channel to decrease towards the edge (Figures 11–13). In doing so, the area in which values that were close to the maximum occurred was expanded. This means that as the dimensions of the matrix increased, the edge phenomenon weakened. From Formula (2), it follows that for matrix dimensions going to infinity, the maximum value of the derivative should tend towards zero. A zero value of the derivative means that the spatial distribution of the number of nodes forming the percolation threshold becomes a constant value. An increase in the dimensions of the matrix also results in a decreasing value of the standard deviation of the percolation threshold, as in Formula (3). From Formula (3) for the standard deviation, it can be seen that this value can, with a good approximation, be described by the relation:

$$\sigma(L) \approx \sigma_0 L^{-0.75}. \tag{3}$$

On the other hand, the maximum value of the rate of reduction in the concentration of nodes, interrupting the last percolation (derivative) channel, is described by the formula:

$$K(L) \approx K_0 L^{-1} \tag{4}$$

A comparison of Formulas (3) and (4) shows that both parameters decrease as the dimensions of the square matrix L increases. This means that both the values of the standard deviation of the percolation threshold and the edge phenomenon are clearly related to the dimensions of the matrix. From Formulas (3) and (4), it can be seen that with increasing matrix dimensions, the edge phenomenon will gradually disappear, and the percolation threshold standard deviation values caused by it will tend towards zero.

4. Conclusions

In this paper, an in-depth analysis of the percolation phenomenon for square matrices with dimensions from $L = 50$ to 600 for 5×10^4 samples was performed using Monte Carlo computer simulations. In the study, the inverse logic of the simulation was used, which is that initially the matrix is completely filled with conducting nodes. The percolation threshold will be reached when the last percolation channel connecting the top and bottom edges of the matrix is broken. This will result in the disappearance of the DC flow between the upper and lower edges of the matrix. The value of the percolation threshold was defined as the quantity of nodes capable of conducting, remaining in the matrix before drawing the node interrupting the last percolation channel, related to the total number of nodes in the matrix.

On the basis of the simulations, it was determined that the distributions of percolation threshold values were normal distributions. Using this foundation, we explored how the expected (average) percolation threshold value and the standard deviation were influenced by variations in matrix dimensions. The study revealed that the average percolation threshold value remained largely unaltered by changes in matrix size.

It was found that the decrease in the standard deviation value of the percolation threshold observed in the study with increasing matrix dimensions is related to the occurrence of the edge phenomenon. The observed reduction in the standard deviation value of the percolation threshold, as the matrix dimensions increased, was associated with the presence of the edge phenomenon. The dependence of the standard deviation value on the matrix dimensions was determined, as well as the dependences describing the spatial distributions of the nodes interrupting the last percolation channel. It can be seen from the determined relationships that with increasing matrix dimensions, the edge phenomenon should gradually disappear and the percolation threshold standard deviation values caused by it will tend towards zero.

References

1. Osetsky, Y.; Barashev, A.V.; Zhang, Y. Sluggish, Chemical Bias and Percolation Phenomena in Atomic Transport by Vacancy and Interstitial Diffusion in Ni Fe Alloys. *Curr. Opin. Solid State Mater. Sci.* **2021**, *25*, 100961. [CrossRef]
2. Jiang, J.; Yu, X.; Lin, Y.; Guan, Y. PercolationDF: A Percolation-Based Medical Diagnosis Framework. *Math. Biosci. Eng.* **2022**, *19*, 5832–5849. [CrossRef]
3. Sahimi, M. Percolation in Biological Systems. In *Applied Mathematical Sciences (Switzerland)*; Springer: Berlin/Heidelberg, Germany, 2023; Volume 213, pp. 443–488.
4. Devpura, A.; Phelan, P.E.; Prasher, R.S. Percolation Theory Applied to the Analysis of Thermal Interface Materials in Flip-Chip Technology. In Proceedings of the Seventh Intersociety Conference on Thermal and Thermomechanical Phenomena in Electronic Systems—ITHERM 2000 (Cat. No.00CH37069), Las Vegas, NV, USA, 23–26 May 2000; Volume 1, pp. 21–28.
5. Evseev, V.A.; Konopleva, R.F.; Skal, A.S. Percolation in Semiconductors with Disordered Regions: Electrical Conductivity and Hall Coefficient. *Radiat. Eff.* **1982**, *66*, 167–172. [CrossRef]
6. Bychkov, E.; Tveryanovich, Y.; Vlasov, Y. *Ion Conductivity and Sensors*; Argonne National Lab: Argonne, IL, USA, 2004; pp. 103–168.
7. Rubie, D.C.; Nimmo, F.; Melosh, H.J. Formation of Earth's Core. In *Treatise on Geophysics*; Elsevier: Amsterdam, The Netherlands, 2007; pp. 51–90.
8. Peng, H.; Sun, X.; Weng, W.; Fang, X. Electronic Polymer Composite. In *Polymer Materials for Energy and Electronic Applications*; Academic Press: Cambridge, MA, USA, 2017; pp. 107–149. [CrossRef]
9. Sulaberidze, V.S.; Skorniakova, E.A. Phenomenon of the Percolation in Composite Materials Based on a Polymer Binder with a Dispersed Filler Phase. *IOP Conf. Ser. Mater. Sci. Eng.* **2020**, *919*, 022009. [CrossRef]
10. Essam, J.W. Percolation Theory. *Rep. Progress Phys.* **1980**, *43*, 833–912. [CrossRef]
11. Hammersley, J.M. A Generalization of McDiarmid's Theorem for Mixed Bernoulli Percolation. *Math. Proc. Camb. Philos. Soc.* **1980**, *88*, 167–170. [CrossRef]
12. Broadbent, S.R.; Hammersley, J.M. Percolation Processes. *Math. Proc. Camb. Philos. Soc.* **1957**, *53*, 629–641. [CrossRef]
13. Carreau, P.J.; Vergnes, B. Rheological Characterization of Fiber Suspensions and Nanocomposites. In *Rheology of Non-Spherical Particle Suspensions*; Elsevier: Amsterdam, The Netherlands, 2015; pp. 19–58.
14. Lebrecht, W.; Centres, P.M.; Ramirez-Pastor, A.J. Empirical Formula for Site and Bond Percolation Thresholds on Archimedean and 2-Uniform Lattices. *Phys. A Stat. Mech. Its Appl.* **2021**, *569*, 125802. [CrossRef]
15. Shlyakhtich, M.; Prudnikov, P. Monte Carlo Simulation of the Critical Behavior near the Percolation Threshold with Invaded Cluster Algorithm. *J. Phys. Conf. Ser.* **2021**, *1740*, 012009. [CrossRef]
16. Dean, P. A New Monte Carlo Method for Percolation Problems on a Lattice. *Math. Proc. Camb. Philos. Soc.* **1963**, *59*, 397–410. [CrossRef]
17. Dean, P.; Bird, N.F. Monte Carlo Estimates of Critical Percolation Probabilities. *Math. Proc. Camb. Philos. Soc.* **1967**, *63*, 477–479. [CrossRef]
18. Derrida, B.; Stauffer, D. Corrections to Scaling and Phenomenological Renormalization for 2-Dimensional Percolation and Lattice Animal Problems. *J. Phys.* **1985**, *46*, 1623–1630. [CrossRef]
19. De Oliveira, P.M.C.; Nóbrega, R.A.; Stauffer, D. Corrections to Finite Size Scaling in Percolation. *Braz. J. Phys.* **2003**, *33*, 616–618. [CrossRef]
20. Jacobsen, J.L. Critical Points of Potts and O(*N*) Models from Eigenvalue Identities in Periodic Temperley–Lieb Algebras. *J. Phys. A Math. Theor.* **2015**, *48*, 454003. [CrossRef]
21. Mertens, S. Exact Site-Percolation Probability on the Square Lattice. *J. Phys. A Math. Theor.* **2022**, *55*, 334002. [CrossRef]
22. Newman, M.E.J.; Ziff, R.M. Efficient Monte Carlo Algorithm and High-Precision Results for Percolation. *Phys. Rev. Lett.* **2000**, *85*, 4104–4107. [CrossRef]
23. Novoselov, K.S.; Geim, A.K.; Morozov, S.V.; Jiang, D.; Zhang, Y.; Dubonos, S.V.; Grigorieva, I.V.; Firsov, A.A. Electric Field Effect in Atomically Thin Carbon Films. *Science* **2004**, *306*, 666–669. [CrossRef] [PubMed]
24. Berger, C.; Song, Z.; Li, T.; Li, X.; Ogbazghi, A.Y.; Feng, R.; Dai, Z.; Marchenkov, A.N.; Conrad, E.H.; First, P.N.; et al. Ultrathin Epitaxial Graphite: 2D Electron Gas Properties and a Route toward Graphene-Based Nanoelectronics. *J. Phys. Chem. B* **2004**, *108*, 19912–19916. [CrossRef]
25. Naguib, M.; Kurtoglu, M.; Presser, V.; Lu, J.; Niu, J.; Heon, M.; Hultman, L.; Gogotsi, Y.; Barsoum, M.W. Two-Dimensional Nanocrystals Produced by Exfoliation of Ti_3AlC_2. *Adv. Mater.* **2011**, *23*, 4248–4253. [CrossRef]
26. Naguib, M.; Mashtalir, O.; Carle, J.; Presser, V.; Lu, J.; Hultman, L.; Gogotsi, Y.; Barsoum, M.W. Two-Dimensional Transition Metal Carbides. *ACS Nano* **2012**, *6*, 1322–1331. [CrossRef]
27. Mashtalir, O.; Naguib, M.; Mochalin, V.N.; Dall'Agnese, Y.; Heon, M.; Barsoum, M.W.; Gogotsi, Y. Intercalation and Delamination of Layered Carbides and Carbonitrides. *Nat. Commun.* **2013**, *4*, 1716. [CrossRef]
28. Ling, Z.; Ren, C.E.; Zhao, M.-Q.; Yang, J.; Giammarco, J.M.; Qiu, J.; Barsoum, M.W.; Gogotsi, Y. Flexible and Conductive MXene Films and Nanocomposites with High Capacitance. *Proc. Natl. Acad. Sci. USA* **2014**, *111*, 16676–16681. [CrossRef]
29. Li, X.; Zhu, H. Two-Dimensional MoS_2: Properties, Preparation, and Applications. *J. Mater.* **2015**, *1*, 33–44. [CrossRef]
30. Bhimanapati, G.R.; Glavin, N.R.; Robinson, J.A. 2D Boron Nitride. In *Semiconductors and Semimetals*; Academic Press Inc.: Cambridge, MA, USA, 2016; Volume 95, pp. 101–147.

31. Shahzad, F.; Alhabeb, M.; Hatter, C.B.; Anasori, B.; Man Hong, S.; Koo, C.M.; Gogotsi, Y. Electromagnetic Interference Shielding with 2D Transition Metal Carbides (MXenes). *Science* **2016**, *353*, 1137–1140. [CrossRef] [PubMed]
32. Akhtar, M.; Anderson, G.; Zhao, R.; Alruqi, A.; Mroczkowska, J.E.; Sumanasekera, G.; Jasinski, J.B. Recent Advances in Synthesis, Properties, and Applications of Phosphorene. *NPJ 2D Mater. Appl.* **2017**, *1*, 5. [CrossRef]
33. Zhen, Z.; Zhu, H. Structure and Properties of Graphene. In *Graphene*; Elsevier: Amsterdam, The Netherlands, 2018; pp. 1–12.
34. Xu, Z. Fundamental Properties of Graphene. In *Graphene*; Elsevier: Amsterdam, The Netherlands, 2018; pp. 73–102.
35. Gogotsi, Y.; Anasori, B. The Rise of MXenes. *ACS Nano* **2019**, *13*, 8491–8494. [CrossRef] [PubMed]
36. Kim, S.; Gholamirad, F.; Yu, M.; Park, C.M.; Jang, A.; Jang, M.; Taheri-Qazvini, N.; Yoon, Y. Enhanced Adsorption Performance for Selected Pharmaceutical Compounds by Sonicated $Ti_3C_2T_X$ MXene. *Chem. Eng. J.* **2021**, *406*, 126789. [CrossRef]
37. Kołtunowicz, T.N.; Gałaszkiewicz, P.; Kierczyński, K.; Rogalski, P.; Okal, P.; Pogrebnjak, A.D.; Buranich, V.; Pogorielov, M.; Diedkova, K.; Zahorodna, V.; et al. Investigation of AC Electrical Properties of MXene-PCL Nanocomposites for Application in Small and Medium Power Generation. *Energies* **2021**, *14*, 7123. [CrossRef]
38. Diedkova, K.; Pogrebnjak, A.D.; Kyrylenko, S.; Smyrnova, K.; Buranich, V.V.; Horodek, P.; Zukowski, P.; Koltunowicz, T.N.; Galaszkiewicz, P.; Makashina, K.; et al. Polycaprolactone-MXene Nanofibrous Scaffolds for Tissue Engineering. *ACS Appl. Mater. Interfaces* **2023**, *15*, 14033–14047. [CrossRef]
39. Zukowski, P.; Okal, P.; Kierczynski, K.; Rogalski, P.; Borucki, S.; Kunicki, M.; Koltunowicz, T.N. Investigations into the Influence of Matrix Dimensions and Number of Iterations on the Percolation Phenomenon for Direct Current. *Energies* **2023**, *16*, 7128. [CrossRef]
40. Zukowski, P.; Okal, P.; Kierczynski, K.; Rogalski, P.; Bondariev, V. Analysis of uneven distribution of nodes creating a percolation channel in matrices with translational symmetry for direct current. *Energies* **2023**, *16*, 7647. [CrossRef]